Journal of Chromatography A, 1513 (2017) 107–117

Contents lists available at ScienceDirect

Journal of Chromatography A

journal homepage: www.elsevier.com/locate/chroma

Biomonitoring of fluoroalkylated substances in Antarctica seabird plasma: Development and validation of a fast and rugged method using on-line concentration liquid chromatography tandem mass spectrometry

Gabriel Munoz[a], Pierre Labadie[b], Emmanuel Geneste[a], Patrick Pardon[a], Sabrina Tartu[c], Olivier Chastel[c], Hélène Budzinski[b,*]

[a] University of Bordeaux, EPOC, UMR 5805, LPTC Research Group, Talence F-33400, France
[b] CNRS, EPOC, UMR 5805, LPTC Research Group, Talence F-33400, France
[c] Centre d'Etudes Biologiques de Chizeí (CEBC), UMR 7372-ULR CNRS, Villiers-en-Bois F-79360, France

ARTICLE INFO

Article history:
Received 9 March 2017
Received in revised form 25 June 2017
Accepted 7 July 2017
Available online 10 July 2017

Keywords:
Polyfluoroalkyl substances
Antarctica
Biomonitoring
Seabird
Plasma
On-line solid phase extraction
Method validation

ABSTRACT

We report on a fast, accurate and rugged analytical procedure to determine a wide span of perfluoroalkyl and polyfluoroalkyl substances (PFASs) in seabird plasma. The 26 investigated compounds included perfluoroalkyl carboxylates (C_5–C_{14} PFCAs), perfluoroalkyl sulfonates (C_4, C_6, C_7, C_8, C_{10} PFSAs), perfluorooctane sulfonamide (FOSA) and N-alkyl derivatives (MeFOSA, EtFOSA), N-alkyl perfluorooctane sulfonamido acetic acids (MeFOSAA, EtFOSAA), fluorotelomer sulfonates (4:2 FTSA, 6:2 FTSA, 8:2 FTSA), polyfluoroalkyl phosphate diesters (diPAPs) and perfluorooctane sulfonamide phosphate diester (diSAmPAP). The method described herein requires a reduced sample amount (25 μL) and involves rapid and simple sample preparation (protein precipitation with acetonitrile but without acidification) prior to analysis by on-line solid phase extraction (Oasis HLB sorbent) coupled to high performance liquid chromatography negative electrospray ionization tandem mass spectrometry. The optimization was conducted using experimental designs to account for potential interactions between variables. Out of the 26 target analytes, 23 compounds showed excellent accuracy (±25% of the expected values). Intermediate precision and matrix effects remained acceptable for most analytes thanks to efficient internal standardization. A human serum standard reference material (NIST SRM 1957) was included in the validation scheme to evaluate method trueness, which proved satisfactory (|Z-scores|<2 for most compounds). Notwithstanding the small initial sample intake, limits of detection as low as 0.003–0.1 ng g^{-1} plasma were obtained. This allowed the determination of 11 target PFASs in Antarctic seabird plasma samples. ΣPFASs in Antarctic seabird plasma ranged from 0.37 to 19 ng g^{-1}, with a predominance of PFOS (>54% of ΣPFASs on average). The reduced plasma amount required implies that the present method could also be applied to the analysis of PFASs in the plasma of smaller biological models.

1. Introduction

The ubiquitous presence of perfluoroalkyl and polyfluoroalkyl substances (PFASs) in all environmental media has been reported and is of growing concern. PFASs are man-made fluoroalkylated chemicals that have been manufactured and used for decades for their excellent surfactant and enduring properties [1]. Since the first papers raised awareness of the widespread occurrence of perfluorooctane sulfonate (PFOS) in wildlife and humans, further evidence have been regularly adduced to document the persistence, bioaccumulation and toxicity of PFASs [2–5]. In addition, there are strong indications that these compounds may undergo biomagnification within food webs, especially long-chained congeners [6]. This has led to the global phase-out of PFOS by major manufacturers, although PFOS is still produced in some locations, including China [7].

The environmental prevalence of PFASs is not solely limited to high profile sites such as PFAS manufacturing facitilities [8,9], firefighting foam impacted sites [10–12] and anthropized freshwater ecosystems [13–16]. Hence, PFASs have also been reported

* Corresponding author.
E-mail address: helene.budzinski@u-bordeaux.fr (H. Budzinski).

http://dx.doi.org/10.1016/j.chroma.2017.07.024
0021-9673/

in remote areas such as the open ocean [17] or polar regions [18]. Long-range atmospheric transport of volatile precursors and their subsequent degradation to more environmentally persistent forms such as perfluoroalkyl acids (PFAAs) have been postulated to explain the occurrence of PFASs in polar regions, while other plausible hypotheses include direct long-range oceanic transport of ionic PFASs and inputs from local contamination sources (e.g., local airports and research stations) [17,19]. However, the relative contribution of each of these pathways is still elusive. To date, PFAS biomonitoring surveys in polar areas have mainly focused on the Arctic environment [20–23], while fewer studies could report data for Antarctic wildlife, including seabirds [24]. Seabirds are top predators, generally long-lived, which are particularly at risk considering the biomagnification potential of some PFASs. Recent papers have further investigated correlations between PFAS levels in Arctic seabirds and the risk of endocrine disruption, decreased hatching success or developmental impairment [25,26]. Thus, seabirds constitute relevant sentinel organisms to investigate the occurrence and effects of PFASs in polar ecosystems.

Conventional methods to extract PFASs from biological tissues are relatively cumbersome to implement, requiring labor-intensive off-line extraction and clean-up procedures, as well as a significant amount of sample material possibly implying animal sacrifice. In order to protect wildlife, a more conservative approach lies in the use of non-lethal sampling methods (e.g., feather or blood sampling). The off-line extraction method of PFASs from blood proposed by Kannan and coworkers [27] used an ion-pairing extraction technique initially introduced by Hansen et al. [28]. Recent methods have also explored automation of the extraction step for improved precision, for instance through automated off-line solid phase extraction (SPE) [29]. Alternatively, methods based on reduced sample preparation and on-line SPE coupled to high performance liquid chromatography tandem mass spectrometry (HPLC–MS/MS) have been reported, and their suitability for the analysis of PFASs in human biologic fluid samples such as breast milk, serum or plasma has been demonstrated [30–39]. Sample intake volume was typically in the 100–300 μL range, albeit the most recent workflows did venture to the low 25–50 μL volumes [37–39].

The determination of PFASs in complex biological matrixes such as plasma or blood samples remains a delicate art, and the analytical pitfalls that may arise are manifold. Hence, in spite of the acknowledgeable advances offered by the previous workflows [30–39], there would still remain some critical knowledge gaps to be bridged. Biases may indeed occur since the early sample collection and storage stage through unintended sample contamination (false positives) or losses of analytes over time (false negatives). Not to mention the possible impact of storage time –a caveat often overlooked in analytical method validation–, there exist other sources of bias. For instance, recovery losses can occur during the multi-step preparation process, while matrix effects may alter reproducibility of instrumental response. If the analytical methods are not suitably vetted, such biases could therefore greatly impact the results generated.

A brief literature review of previous works for the determination of PFASs in human serum/plasma via on-line SPE – liquid chromatography mass spectrometry was conducted [30–39]. An optimization of chromatographic conditions was conducted in at least 7/10 studies. The most commonly studied parameter was the analytical mobile phase composition (i.e. buffer type and concentration) that can play an essential role in analyte elution from the SPE column and through the analytical column as well as in ionization performance [31,34–39]. Interestingly, fewer studies (1/10) examined the influence of on-line SPE loading conditions on analyte response, such as sample loading flow rate and sample injection volume [37]. In the aforementioned reference –and general on-line SPE literature for other organic contaminants, for that matter– such parameters were varied using one-variable-at-a-time designs. Hence, the existence of interactions has been previously overlooked even though such parameters may not be independent, which constituted a first important knowledge gap with regard to separation science. The usual validation endpoints were documented in 10/10 studies, addressing linearity range and correlation (R) or determination (R^2) coefficients, precision, and accuracy. Somewhat inconclusive linearity performance was reported in some instances ($R^2 \sim 0.98$); this, in turn, may preclude a reliable quantification at sub part-per-billion levels. Additionally, the low volumes of isotope-labelled internal standards that are initially spiked to the samples may lead to irreproducible results when operating under volumetric addition. A similar comment would in fact apply to the addition of low volumes of plasma/blood samples, due to the viscosity of the undiluted matrix. Gao et al. [37] have urged prudence regarding this phenomenon that could lead to irreproducible results at the later instrumental stage. Hence, the authors advocated in favor of a suitable sample dilution with ultrapure water prior to LC–MS injection [37]. In the various method developments, the terms of “accuracy” and “recovery” were often used interchangeably, although strictly speaking they do not capture the same reality. Analytical trueness is another endpoint that is rarely included in method validation; based on the present review, only 3/10 studies analyzed reference samples. A detailed matrix effect study was only included in 2/10 papers. This could yield conflicting results, should a solvent-based calibration be implemented in further method applications.

In view of the aforestated limitations, the overarching aim of the present study was to propose a sensitive, rapid, and robust method for the determination of 26 PFASs in Antarctic seabird plasma. Compared to previous reports [30–39], a wider breadth of PFAS chain lengths and chemistries could be accommodated with limited sample pre-treatment and within a single on-line SPE HPLC–MS/MS method. A further specific objective was to operate at very low sample intake notwithstanding the low anticipated PFAS concentration in the samples. The low intake volumes would hence allow future transferability of the biomonitoring method to smaller biological models. In that respect, the use of experimental design methodologies was critical in order to identify suitable on-line SPE operating conditions; to the authors’ best knowledge, a stringent cross-factor optimization of the loading step was not previously reported in any on-line SPE study. In view of the low plasma sample volume selected (25 μL), a noteworthy improvement was to operate a systematic control of the additions of isotope-labelled ISs and plasma samples gravimetrically. The concentrations reported in the present study were thus expressed on a mass basis, rather than on a volume basis. Taken together, these aspects contributed to maintaining excellent whole method performance. The method was successfully validated by evaluating detection limits, linearity, sample preparation recovery, precision, and accuracy on fortified chicken plasma. Raw matrix effects were evaluated in chicken plasma samples and real seabird plasma alike, through the examination of isotope-labelled internal standards, while the effective matrix effects were evaluated upon comparison of the slopes of the solvent-based and matrix-matched calibration curves. The analysis of a human serum standard material (NIST SRM 1957) was also included to assess method trueness. Finally, since a few months typically elapsed between the plasma sample collection in the Antarctica continent and subantarctica islands and their analysis, the influence of storage time was investigated over a 6-month period. The method was successfully applied to a selection of seabird plasma samples, providing valuable insights into the occurrence of legacy and emerging PFASs in Antarctic biota.

2. Experimental

2.1. Chemicals and standards

Solutions of native PFASs had chemical purities greater than 98% for individual compounds and were all acquired from Wellington Laboratories (BCP Instruments, Irigny, France). Target molecules included 10 PFCAs (PFPeA, PFHxA, PFHpA, PFOA, PFNA, PFDA, PFUnDA, PFDoDA, PFTrDA and PFTeDA), 5 PFSAs (PFBS, PFHxS, PFHpS, linear PFOS (L-PFOS) and PFDS), perfluorooctane sulfonamide (FOSA) and its N-alkylated derivatives (MeFOSA and EtFOSA), N-alkylated perfluorooctane sulfonamido acetic acids (MeFOSAA and EtFOSAA), fluorotelomer sulfonates (4:2 FTSA, 6:2 FTSA and 8:2 FTSA), and polyfluoroalkyl phosphate diesters (6:2 diPAP, 8:2 diPAP) and perfluorooctane sulfonamide phosphate diester (diSAmPAP). For perfluorooctane sulfonate branched isomers (Br-PFOS), concentrations were calculated from the calibration curve used for L-PFOS. Solutions of isotopically labelled compounds (internal standards, ISs) had chemical purities greater than 98% and isotopic purities greater than 99%, and were all purchased from Wellington Laboratories. $^{13}C_2$-PFHxA, $^{13}C_4$-PFOA, $^{13}C_2$-PFDA, $^{13}C_2$-PFUnDA, $^{13}C_2$-PFDoDA, $^{13}C_2$-PFTeDA, $^{18}O_2$-PFHxS, $^{13}C_4$-PFOS, D_3-N-MeFOSAA, $^{13}C_8$-FOSA, D_3-N-MeFOSA, D_5-N-EtFOSA, $^{13}C_2$-6:2 FTSA and $^{13}C_4$-6:2 diPAP were used as ISs. Full names and structures of target analytes are supplied in the Supporting Information (SI) (**Table S1**).

Methanol (MeOH), acetonitrile (ACN) and HPLC-water (Baker analyzed LC–MS reagent) were from J.T. Baker (Atlantic Labo, Bruges, France). Ammonium acetate (CH_3COONH_4) for HPLC (≥99.0%) was from Sigma-Aldrich (S^t Quentin Fallavier, France) while formic acid (HCOOH) (≥99.0%, LC–MS reagent) was from J.T. Baker (Deventer, Netherlands). Costar 2 mL polypropylene centrifuge tubes (0.22 μm nylon filter) were from Corning Incorporated (NY, USA). Oasis HLB on-Line SPE columns (2 × 10 mm, d_p = 25–35 μm) were from Waters (Guyancourt, France) while on-Line PLRP-S columns (2.1 × 12.5 mm, d_p = 15–20 μm) were from Agilent Technologies (Massy, France). Chicken plasma was acquired from Sigma-Aldrich (S^t Quentin Fallavier, France).

2.2. Sample collection

South polar skua (*Stercorarius maccormicki*) and snow petrel (*Pagodroma nivea*) plasma samples were collected at Adelie Land (French Antarctic Territory Terre Adélie, Antarctica, 66°40′S, 140°01′E), while king penguin (*Aptenodytes patagonicus*) plasma samples were sampled at Ile de la Possession (French Antarctic Territory Crozet Island, Subantarctic Islands, 46°24′S, 51°45′E) in 2013. All samples were collected from chick-rearing adults. An overview of the sampling areas is presented in the SI (**Fig.S1**). Blood samples were collected from the alar vein with a heparinized syringe, centrifuged, and plasma was finally recovered and stored in polypropylene tubes at −20 °C until further analysis.

2.3. Sample preparation and analysis

A 25 μL aliquot of plasma was weighed (~25 mg) in 2 mL polypropylene Eppendorf tubes, and ISs were subsequently added under gravimetric control (~25 mg of a 1 pg μL^{-1} IS mixture prepared in methanol). Following protein precipitation with 100 μL of ACN, extracts were centrifuged (24,000*g*, 10 min) and the supernatant was transferred to 2 mL polypropylene centrifuge tubes (0.22 μm nylon filter). Following centrifugation of the latter (7000*g*, 3 min), extracts were finally transferred to 2 mL auto sampler glass vials and diluted with ~675 μL of HPLC-water. Extracts were briefly vortexed and then processed using an Agilent Technologies (Massy, France) on-line SPE platform which comprises a standard auto sampler (1260 Infinity ALS), a quaternary pump (1260 Infinity Quaternary Pump VL), a switch valve (1200 2 Position/6 Port Valve) and an on-line SPE column support (1200 6 Position Selection Valve), all of which were automatically controlled via the Acquisition module of the Agilent Mass Hunter software. Sample enrichment by on-line SPE was achieved as follows: after sampling 400 μL of extract by the auto sampler, extracts are loaded at 600 μL min^{-1} onto an Oasis HLB on-line SPE column. The switch valve is then commuted and analytes are eluted in back-flush mode at 300 μL min^{-1} and transferred onto an analytical column (Agilent C18 Poroshell, 2.1 × 100 mm, 2.7 μm). Ionization and detection were achieved by an electrospray ionization interface (negative mode) and a 6490 triple quadrupole mass spectrometer (Agilent Technologies) operated in dynamic multiple reaction monitoring mode. To extend the life time of the analytical column and prevent gradual clogging of the latter, an Agilent Poroshell 120 SB C18 guard column (2.1 × 5 mm, 2.7 μm) was connected to the analytical column inlet. Also note that a Zorbax SB C18 column (2.1 × 30 mm, 3.5 μm) was used as a trap to remove potential PFAS contamination originating from the aqueous mobile phase; it was positioned immediately at the aqueous pump exit and before the mixing point with the second pump channel [14]. On-line SPE and analytical gradient conditions are provided in the SI (**Table S2**), as well as further details regarding mass spectrometry acquisition parameters for ISs and native analytes (**Tables S3-S4**).

2.4. Method optimization

An exploratory test was first conducted in HPLC-water samples spiked at 15 pg mL^{-1} to select the SPE sorbent (HLB *Vs* PLRP-S) and to investigate the effect of formic acid addition to the samples (0.1% HCOOH v/v) (pH ~2.6) on analyte retention. For this preliminary experiment, the loading volume was fixed at 300 μL while the sample transfer rate from the injection loop to the on-line SPE column (loading speed) was set at 600 μL min^{-1}. The residual organic solvent percentage resulting from spiking native analytes into HPLC-water was approximately 0.1% (v/v). Following the choice of adequate on-line SPE column and pH conditions, complementary experiments were run with spiked matrix-free samples to evaluate the combined influence of organic solvent percentage (MeOH or ACN) (% of organic modifier in HPLC-water varied between 0.1 and 12.5% v/v) and on-line SPE loading volume (varied between 200 and 800 μL) on analyte retention. Combinations were studied through a full factorial experimental design.

The choice of the protein precipitation solvent was conducted using unspiked seabird plasma samples. For each matrix type (namely, snow petrels, king penguins and skuas), 25 μL aliquots of plasma were submitted to the procedure described in **2.3**, the protein precipitation solvent being either ACN (n = 3) or MeOH (n = 3). Internal standards were added post-sample preparation to evaluate differences in ionization suppression or enhancement between the two procedures.

On-line SPE loading speed and loading volume were highly likely to interact. The latter were therefore optimized simultaneously, using a full factorial design. Loading speed was varied between 200 and 1000 μL min^{-1} and loading volume between 200 and 600 μL. Each combination was analyzed in triplicate and during the same working day, but run in random order to attenuate the impact of lurking variables [40,41]. These tests were performed on a pool of chicken plasma samples prepared as described in **2.3** (except for IS addition), spiked post-preparation at 120 pg mL^{-1} with native analytes and subsequently aliquoted.

2.5. Method validation

For validation purposes, a chicken plasma matrix with non-detectable PFAS analytes was used as a proxy for seabird plasma matrix.

Analyte recovery during sample preparation was assessed at two fortification levels (0.5 and 5 ng g^{-1} plasma), in quintuplicate. For each replicate, recovery (expressed in%) was calculated using Eq. (1):

$$\text{Preparationrecovery} = 100 \times S_{Before}/S_{After} \quad (1)$$

with S_{Before} the analyte to IS area ratio (corrected by the analyte to IS mass ratio) observed in a chicken plasma aliquot spiked before sample preparation with native analytes (ISs being added post-sample preparation) and S_{After} the mean (n = 3) analyte to IS area ratio (corrected by the analyte to IS mass ratio) in chicken plasma samples spiked post-sample preparation with native analytes jointly with ISs. Using this methodology, the recoveries reported should not be excessively affected by matrix effects [11,41].

Method precision was also evaluated at two fortification levels (0.5 and 5 ng g^{-1} plasma) by spiking target analytes jointly with mass-labelled ISs at the beginning of the preparation procedure. Therefore, the reported precision accounted for the variability inherent to both sample preparation and instrumental analysis. Intra-day precision was calculated as the relative standard deviation of 5 replicates prepared and analyzed on the same working day. This process was repeated for 3 replicates on a second and third working day and inter-day precision derived from the overall relative standard deviation (n = 11).

Method accuracy was evaluated by replicate analyses of chicken plasma samples spiked at two different concentrations (0.5 and 5 ng g^{-1}, n = 5 for each level), quantified against a solvent-based calibration curve, and expressed as a percentage of the expected value. Since the addition of native analytes and ISs occurred at the start of the preparation procedure, these quality controls in fact correspond to whole method accuracy, thereby integrating potential biases (e.g., recovery losses, matrix effects). Additionally, method trueness was assessed through the measurement of a human serum standard reference material (NIST SRM 1957).

Linearity was examined through a two-fold approach, one solvent-based and one by standard additions of analytes to chicken plasma (spiked post-sample preparation). In both cases, 10-point calibration curves were built, the IS mass added being kept constant and the levels used for target analytes ranging between 0.02 and 40 ng g^{-1} plasma (extrapolated on the basis of a 25 mg aliquot of plasma sample). Also note that the final aqueous/organic solvent ratio used for plasma samples was respected for all calibration levels and quality controls, since the residual organic percentage in final extract was shown in the earlier optimization stage to be an influential variable of analyte response (see also Section 3.1). Analyte to IS area response ratios were plotted against analyte to IS concentration ratio by using linear models (1/x weighted regression). The matrix effect on the whole concentration range was finally evaluated by comparing the regression slope obtained by the two approaches.

2.6. Quality control and data analysis

HPLC-water aliquots (n = 20) were run between each seabird plasma samples, and contained low yet detectable amounts of 6:2 diPAP, PFUnDA and FOSA (estimated amounts of 2.6, 0.23 and 0.011 pg on-column, respectively). Injection blank replicates were very reproducible; in addition, PFOS (the dominant compound in seabird plasma samples) was not detected in these injection blanks, suggesting minimal carryover. This implies that samples can be injected consecutively without any risk of cross-contamination, increasing overall sample throughput.

A total of 12 procedural blanks were analyzed, and consisted of 25 μL of HPLC-water that went through the entire analytical procedure. PFOA, FOSA and 6:2 diPAP were systematically detected, and PFUnDA or PFHpA also frequently reported (10/12). Other analytes such as PFHxA, PFDA or PFTrDA were only found sporadically (3/12) (see SI **Table S5** for full details).

For those analytes found in procedural blanks, levels were blank-corrected and the limits of detection (LODs) were determined as the standard deviation of the blanks multiplied by the $t_{n-1,95}$ student coefficient, with n the number of blank replicates [14,42]. Otherwise, the LOD was derived from the signal-to-noise ratio (SNR) observed in either low-contaminated seabird plasma samples (typically, 0.1–1 ng g^{-1} plasma) or in chicken plasma samples spiked at 0.5 ng g^{-1}. When two transitions were followed (quantitation and confirmation), the transition with the lowest SNR was chosen for LOD calculation (SNR = 3). The limit of quantification (LOQ) was then defined as the most stringent of the two following approaches: (i) calculated as 3 x LOD or (ii) set at the lowest acceptable level of the calibration curve.

Positive identification of target analytes was based on matching retention times (tolerance: ±2.5%) with a reference standard, SNR > 3 for both quantitation (Q) and confirmation (C) transitions, when applicable, and a Q/C response ratio deviating <25% from the expected value.

Statistics were performed with the Sigmaplot™ 11.0 (Systat Software) and R statistical software (R version 2.15.3, R Core Team, 2013). Statistical significance was defined as $p < 0.05$.

3. Results and discussion

3.1. Optimization of sample preparation and on-line SPE settings

Sample preparation and analytical operating conditions should be carefully designed to elicit maximum analyte recovery and yield the finest possible LODs. In the initial stages of the optimization process, the influence of sample pH and on-line SPE polymeric phase nature were jointly investigated (see Section 2.4). Addition of formic acid to the samples (0.1% v/v) had a significant positive impact on analyte signal for short-chain compounds (e.g., short-chain PFCAs such as PFPeA), possibly as a consequence of a better retention of the latter on the on-line SPE column (increase of the proportion of these analytes in their neutral form) (Fig. 1). While acidic conditions (pH ~ 2.6) had little influence on signal intensity for compounds such as C_7–C_8 PFCAs, 6:2 FTSA or PFHxS, analyte signal dropped sharply for longer-chain PFASs such as PFOS or PFUnDA (three-fold and ten-fold decrease, respectively). The signal decrease observed for long-chain PFCAs (pKa ~ 3-4) may be ascribed to the increase of the proportion of the neutral form, analytes being prone to increased sorption on vial walls or tubings, while that of PFOS is more delicate to explain since it would predominantly occur as the dissociated form (pKa « 0) [43,44]. There is, however, another possibility that may explain the signal decrease of PFOS when the samples were amended with formic acid. It is well known that the HLB sorbent can provide both lipophilic and hydrophobic interactions. Apart from hydrophilicity, the N-vinylpyrrolidone units may provide another feature. After sample amendment with formic acid, electrostatic interactions may indeed happen between PFOS (strong acid) and protonated N-vinylpyrrolidone. This could have led to decreased elution efficiency at the on-line SPE back-flush elution stage compared to non HCOOH-amended samples, resulting in lower apparent recoveries. Addition of formic acid to the samples was therefore discarded, while the HLB sorbent was adopted for the fair signal intensity and precision it produced.

It is also worth elaborating on the effect of residual organic solvent percentage in extracts on analyte signal, since non-negligible volumes of MeOH [33] or ACN [30,34–36] are commonly added to plasma samples to induce protein precipitation. Arguably, a high organic solvent content in the final extract may alter analyte interactions with the on-line SPE polymeric phase if the sample loading

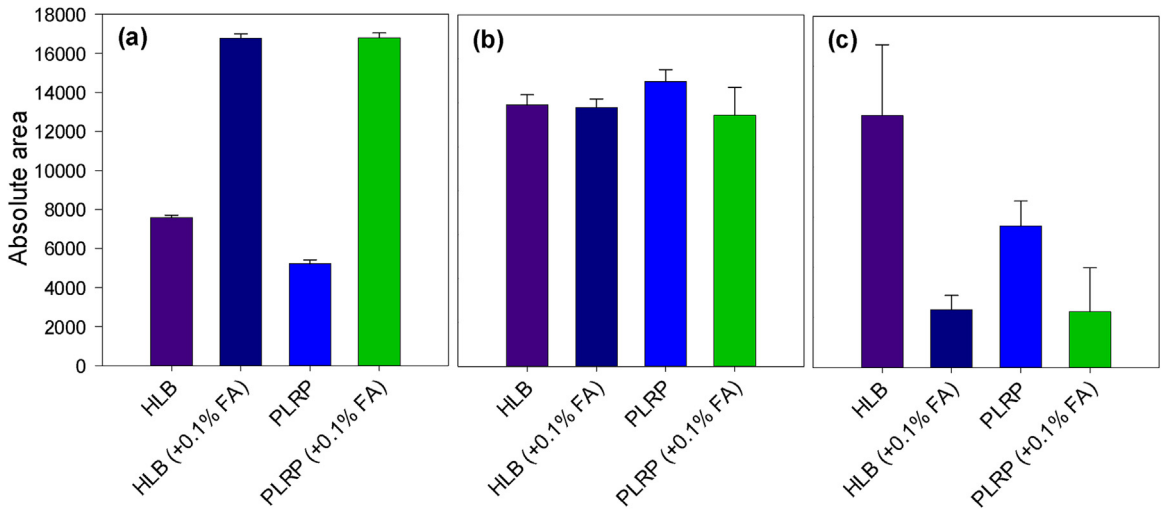

Fig. 1. Effect of on-line SPE sorbent nature and formic acid (FA) addition to the samples on analyte absolute area, illustrated for perfluoroalkyl carboxylates of various chain lengths: **(a)** PFPeA; **(b)** PFOA; **(c)** PFUnDA. Error bars indicate standard deviation (n = 3).

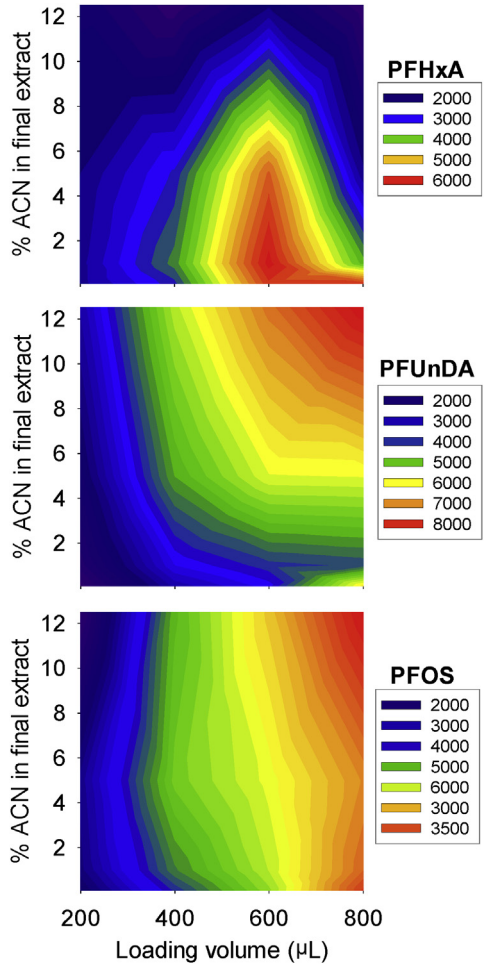

Fig. 2. Influence of on-line SPE loading volume (μL) and organic solvent percentage (% ACN) on analyte absolute area, illustrated for PFHxA, PFUnDA and PFOS.

conditions are poorly designed. In the present study, the influence of MeOH or ACN residual percentage on analyte absolute area was investigated jointly with on-line SPE loading volume (full factorial design). PFCAs displayed different optimal operating zones according to their perfluoroalkyl chain length (Fig. 2). For instance, the retention of PFHxA was hindered for ACN percentages >5%, while no particular trend was observed for PFOA or PFNA for each loading volume considered. Note that similar trends were observed when using MeOH as the organic modifier (SI **Fig.S2**). In contrast, analyte signal concomitantly increased with organic solvent percentage for the most hydrophobic PFCAs (reduction of sorption losses) (e.g., PFUnDA) (Fig. 2). Since the latter could possibly be found in plasma samples owing to their higher bioaccumulative properties, conditions that would promote their detection were selected, namely 12.5% organic solvent. Note that at 12.5% organic solvent, analyte signal generally increased in a linearly fashion up to 600 μL, after which analyte signal either plateaued or dropped. This could reflect the fact that analyte accumulation had reached the dynamic equilibrium (compensation of analyte retention and breakthrough on the on-line SPE sorbent). Hence, loading volume was only investigated in the 200–600 μL range in the optimization of other on-line SPE parameters.

The choice of the protein precipitation solvent was conducted in non-spiked seabird plasma samples. ACN-treated samples generally exhibited higher analyte signal than those treated with MeOH, especially for longer-chain PFASs (SI **Fig.S3**). In addition, the IS signal was slightly superior when using ACN (SI **Fig.S4**). Taken together, these observations suggest that higher recovery and more efficient clean-up may be achieved with ACN, which led to its selection. Note that a small plasma sample size of 25 μL was selected, preliminary experiments having shown that higher sample amounts (i.e. 50 or 100 μL) may lead to significant signal suppression and less robustness (back-pressure increase) when using >200 μL on-line SPE loading volumes.

On-line SPE main parameters (loading speed and loading volume) were finally optimized through a 3^2 full factorial design on spiked chicken plasma (see Section 2.4). Analyte peak shape, intensity and variability were therefore examined for 9 different operating conditions. The existence of interactions between sample loading volume and loading speed is apparent in the response surfaces shown in Fig. 3. For instance, PFUnDA absolute areas remained globally unchanged at 400 μL injection volume regardless of loading flow rate (varied in the range 200–1000 μL min^{-1}), while the impact of flow rate was more pronounced for a higher loading volume. Higher peak areas were generally obtained when combining the lowest loading speed (200 μL min^{-1}) and the highest loading volume (600 μL), with the notable exception of short-chain PFASs (e.g. PFPeA, PFHxA, 4:2 FTSA) for which dramatic signal loss was observed at the lowest flow rates investigated (Fig. 3). We

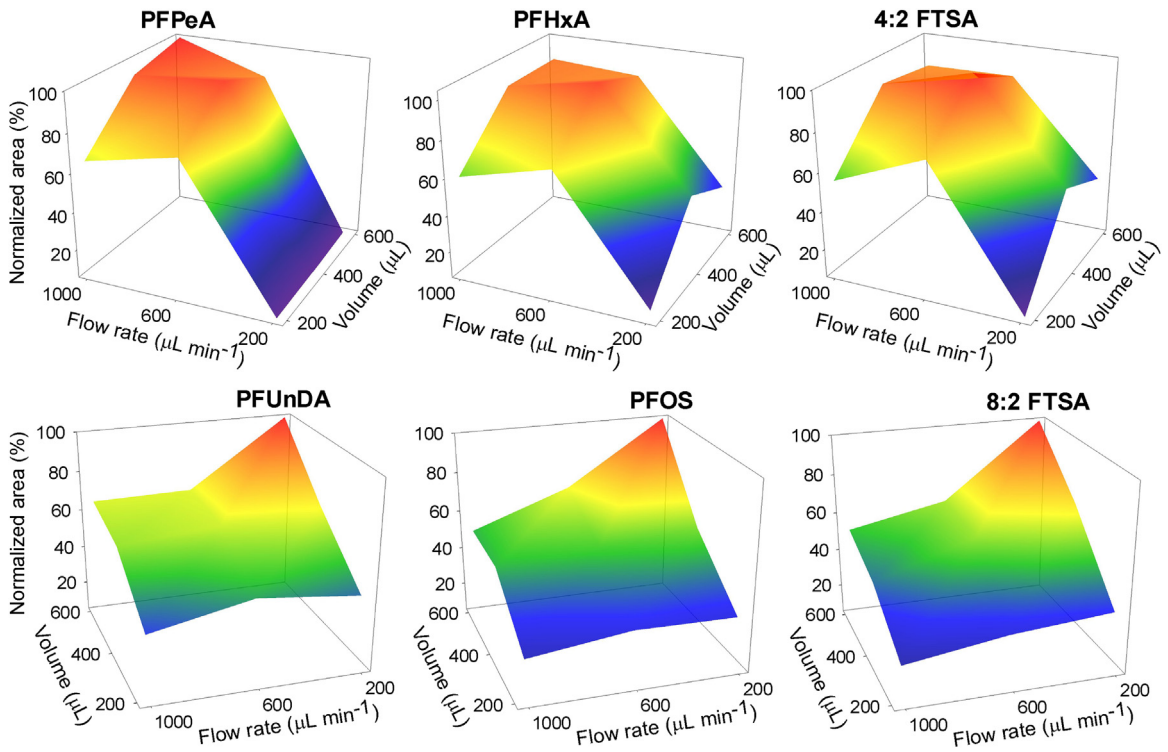

Fig. 3. Combined influence of on-line SPE loading flow rate and loading volume on analyte normalized areas, illustrated for short chain (PFPeA, PFHxA, 4:2 FTSA) and long-chain (PFUnDA, PFOS, 8:2 FTSA) fluoroalkylated acids. For the sake of clarity, a different angle view was selected for short-chain and long-chain PFASs. The diluted chicken plasma matrix was spiked postpreparation at 120 pg mL^{-1} with native analytes (see also Section 2.4).

can surmise that this phenomenon reflects the increased retention of specific matrix interfering components at lower loading speed, which would later cause signal suppression of short-chain PFCAs through competition in the ESI process. Another obvious disadvantage of the 200 μL min^{-1} based-method compared to higher loading speed methods is the lower sample throughput. In order to keep a single analysis method for all target PFASs, the best compromise in terms of analyte response, variability and sample turnaround time was eventually selected at the center point of the design (600 μL min^{-1} and 400 μL).

Using these conditions and a sample amount of 25 μL, no significant back-pressure increase was observed between consecutive injections of seabird plasma samples (n = 21) (SI **Fig.S8**). Another noteworthy advantage of combining a small sample amount and a relatively large on-line SPE loading volume is the reduced amount of ISs required (∼ 30 pg added at the beginning of the preparation procedure, ∼ 100-fold lower than traditional off-line methods), since a large proportion (50%) of final extract is injected.

3.2. Linearity assessment and matrix effects

Ten-point calibration curves (1/x weighted regression) were built for both solvent-based and matrix-based approaches (range tested: 0.02–40 ng g^{-1}). In the solvent-based approach, the linearity range covered by the calibration curve generally spanned 2–3 orders of magnitude (0.1–40 ng g^{-1} plasma equivalent, calculated on the basis of a 25 mg sample amount) with excellent determination coefficients (R^2 range: 0.9924–0.9994) (Table 1). Residuals remained generally between ± 20% of the calculated trend lines, and the deviation observed at the highest calibration level was always < ± 6% (Table 1), suggesting that the linear range may extend beyond 40 ng g^{-1} for most analytes. In the matrix-based standard addition approach, the linear range also spanned 2–3 orders of magnitude (0.1–40 or 0.25–40 ng g^{-1} in most cases), with determination coefficients ≥ 0.9934 (data not shown).

Electrospray ionization being notoriously vulnerable to signal alterations due to endogenous matrix constituents that may co-elute with target analytes, assessment of matrix effects is therefore essential to ensure the validity and reliability of the results [45,46]. The use of adequate mass-labelled ISs can, to some extent, compensate for signal exaltation or suppression and ensure accurate quantitation of target analytes [46,47]. In the present method, the solvent-based and chicken plasma matrix-based calibration curves exhibited similar coefficients (overlapping 95% confidence intervals) (e.g., L-PFOS, SI **Fig.S5**), resulting in moderate matrix effects (-19% to + 12%) for 23/26 target analytes (Table 2). A discrepancy was however observed in the specific case of PFDS (+ 118%), 8:2 diPAP (-61%) and diSAmPAP (−38%), suggesting that $^{13}C_4$-PFOS (for PFDS) or $^{13}C_4$-6:2 diPAP (for 8:2 diPAP and diSAmPAP) did not efficiently compensate for matrix effects. Since the aforementioned analytes were never actually detected in any of the seabird plasma samples, it would be possible to keep the solvent-based calibration curve approach for quantitation purposes. This would yield satisfactory accuracy for most analytes (see also Section 3.3). Should PFDS, 8:2 diPAP or diSAmPAP be found in plasma samples, quantitation may be addressed by standard additions. Alternatively, it may be advantageous to acquire the matching isotope-labelled internal standard, if available.

In addition, the "raw" matrix effect was estimated upon examination of the absolute area of ISs in solvent-based (i.e. procedural blanks) and several plasma samples. Most ISs were either little or not affected by the presence of a matrix (SI **Fig.S6**). $^{13}C_4$-PFOS absolute areas observed in the various matrices remained between − 5 and + 15% of the value observed in the matrix-free solvent, while some particular ISs did not withstand signal suppression ($^{13}C_8$-FOSA) or exaltation ($^{13}C_2$-PFHxA, $^{13}C_2$-PFDA, D_3-N-MeFOSAA) as efficiently.

Table 1
Analytical figures of merit of the calibration curve. Information on the deviation (%) between observed (y) and calculated-back (ŷ) response is also provided.

	Linearity range (ng g^{-1} plasma)	R^2	Deviation at lowest calibration level (%)	Deviation at highest calibration level (%)
PFPeA	0.1–10	0.9933	+11	+0.85
PFHxA	0.1–40	0.9971	−25	−4.2
PFHpA	0.1–40	0.9982	−29	−2.6
PFOA	0.25–40	0.9979	−11	−1.1
PFNA	0.1–40	0.9975	+3.2	−1.9
PFDA	0.1–40	0.9957	+0.79	−5.5
PFUnDA	0.25–40	0.9952	−14	−5.2
PFDoDA	0.1–40	0.9984	+10	+0.34
PFTrDA	0.1–40	0.9956	−18	−3.5
PFTeDA	0.1–40	0.9994	−22	−1.0
PFBS	0.1–40	0.9982	−29	−1.5
PFHxS	0.1–40	0.9980	−18	−4.1
PFHpS	0.02–40	0.9940	−29	+4.1
L-PFOS	0.1–40	0.9992	−14	−1.2
PFDS	0.1–40	0.9924	+16	+2.9
MeFOSAA	0.25–40	0.9947	+2.3	−3.0
EtFOSAA	0.1–40	0.9978	−2.5	−0.39
FOSA	0.02–40	0.9963	−25	+2.2
MeFOSA	0.02–40	0.9970	−9.9	+4.6
EtFOSA	0.02–40	0.9982	+0.26	+1.2
4:2 FTSA	0.25–40	0.9932	+21	−1.4
6:2 FTSA	0.25–40	0.9993	+35	−1.3
8:2 FTSA	0.1–40	0.9940	+28	−0.92
6:2 diPAP	0.75–40	0.9980	−4.8	−1.5
8:2 diPAP	0.75–40	0.9937	+22	+3.9
diSAmPAP	0.75–40	0.9978	−19	+1.3

3.3. Method performance

Table 2 displays the key validation parameters illustrating the method performance. LODs were in the range 0.003–0.1 ng g^{-1} plasma, which is lower than or in the same order of magnitude as previously reported methods [30–39] (Table 3). Recovery, accuracy and precision were evaluated on chicken plasma fortified at 0.5 and 5 ng g^{-1} (see also Section 2.5). Acceptable recoveries were obtained for the method preparation procedure, in the range 46–95% for PFCAs, 68–81% for PFSAs, and 67–124% for other analytes. Intra-day and inter-day precision were assessed on chicken plasma samples spiked with native PFASs at two levels and ranged between 2 and 26% and 3–44%, respectively. Method accuracy was evaluated likewise, and generally remained between ± 20% of the target values, with the noteworthy exception of PFDS, 8:2 diPAP and diSAmPAP due to matrix effects not compensated for by ISs (see also Section 3.2). In addition, a human serum standard reference material (NIST SRM 1957) was analyzed to evaluate method trueness; the concentrations found in both a freshly reconstituted sample and a subsample stored at −18 °C for 6 months were in either reasonable or excellent agreement with the NIST consensus values (Table 4). For most compounds, average Z-scores were lower than 2 (in absolute terms), and even lower than 1 for PFOS. For PFHpA and PFOA, |Z-scores| were occasionally >3. For the former, this may be due to the fact that the sample concentration (NIST reference: 0.31 ng g^{-1} plasma) was close to our reported LOQ (Table 2); for the latter, it may be a consequence of the relatively low standard deviation reported by NIST. It is however germane to note that PFOA and PFHpA determined concentrations were still acceptable, in the range 70–85% and 50–120% of the NIST reference value, respectively (Table 4).

3.4. Intermediate precision and influence of storage time

Haug et al. [33] repeated the intra-day variation assay a few months after the method validation process had been completed to evaluate the intermediate precision of their on-line SPE HPLC–MS/MS method. In the present study, the intra-day precision experiment was repeated six months after the initial validation on spiked chicken plasma samples (0.5 and 5 ng g^{-1}) (n = 5). The intra-day variations obtained were in the range 4–22 and 2–17% for the low and high spike levels, respectively (data not shown), in excellent agreement with the ones obtained in the initial series.

In addition, the freshly reconstituted human serum (NIST SRM 1957) used in our initial validation was stored at − 20 °C for a duration of 6 months to investigate the stability of analytes upon time, since Antarctic seabird plasma samples were typically stored at −20 °C for several months between sampling and analysis. Little influence of storage time was detected, typical deviations after six months of storage oscillating between ± 25% from the initial concentration (Table 4) with the exception of PFHpA. Overall, these observations suggest that after reconstitution of NIST SRM 1957 in HPLC-water and subsequent homogenization, the latter may be divided into small sample aliquots and stored at −20 °C for several months until being thawed anew and used for quality control purposes, without major analyte loss.

3.5. Occurrence of PFASs in Antarctic and Southern Ocean seabirds

The applicability of the newly-developed on-line SPE HPLC–MS/MS method was assessed through the analysis of adult king penguin, snow petrel and South polar skua plasma samples (n = 7 for each species). An illustration of the chromatograms obtained for PFOS in a procedural blank and a South polar skua plasma sample is provided in the SI (**Fig.S7**).

Average PFAS levels are presented in Fig. 4. 11/26 target analytes were detected in the plasma of selected Antarctic and Subantarctic seabird species. ΣPFASs ranged between 0.4 and 19.1 ng g^{-1} plasma. PFOS was generally the dominant compound of the PFAS pattern, at times reaching levels >10 ng g^{-1} plasma (for full details on concentrations, see **Table S6** of the SI). Although South polar skuas and snow petrels were collected at the same location (Adelie Land, Antarctica), ΣPFASs was 1.2–51 times higher for skuas, with notable levels of long-chained PFCAs such as PFUnDA or PFTrDA (in the range 0.84–4.0 and 0.45–1.9 ng g^{-1} plasma, respectively). South polar skuas are long-distance migratory birds [48,49], breeding in Antarctica in the Austral summer and heading northward to winter

Table 2
Method performance: limit of detection (LOD) and limit of quantification (LOQ), sample preparation recovery rates, accuracy, precision, and matrix effect. Tests were conducted on chicken plasma samples spiked at two fortification levels (0.5 and 5 ng g^{-1} plasma). When applicable, standard deviation is given in brackets. Intra-day and inter-day precision correspond to relative standard deviations (n = 5 and 11, respectively).

	LOD* ng g^{-1}	LOQ** ng g^{-1}	Recovery (%)	Recovery (%)	Accuracy (%)	Accuracy (%)	Intra-day precision (%)	Intra-day precision (%)	Inter-day precision (%)	Inter-day precision (%)	Matrix effect (%)
Spike level (ng g^{-1} plasma)			0.5	5	0.5	5	0.5	5	0.5	5	
Replicates			5	5	5	5	5	5	11	11	
PFPeA	0.09[a]	0.27[d]	46 (37)	64 (18)	123 (7)	121 (9)	6	7	32	27	−13
PFHxA	0.07[a]	0.21[d]	76 (5)	71 (7)	100 (5)	85 (10)	5	2	5	3	−7
PFHpA	0.1[a]	0.3[d]	87 (6)	70 (8)	85 (3)	73 (8)	13	12	38	31	−12
PFOA	0.05[a]	0.25[e]	95 (17)	73 (9)	118 (7)	102 (8)	9	4	10	4	−2
PFNA	0.02[b]	0.1[e]	79 (11)	78 (10)	119 (14)	116 (10)	10	20	22	35	+8
PFDA	0.03[a]	0.1[e]	67 (12)	67 (5)	97 (7)	94 (6)	3	6	8	7	−15
PFUnDA	0.05[a]	0.25[e]	90 (10)	69 (6)	101 (11)	97 (2)	5	5	8	8	−17
PFDoDA	0.02[a]	0.1[e]	75 (10)	75 (10)	94 (8)	102 (7)	7	8	8	8	−2
PFTrDA	0.02[a]	0.1[e]	62 (6)	71 (7)	126 (13)	123 (14)	10	11	22	18	−3
PFTeDA	0.003[b]	0.1[e]	66 (5)	69 (3)	93 (15)	103 (12)	13	8	11	9	+5
PFBS	0.004[b]	0.1[e]	78 (3)	68 (2)	79 (6)	84 (1)	3	4	24	25	+2
PFHxS	0.005[b]	0.1[e]	79 (10)	68 (1)	87 (3)	96 (3)	3	2	8	7	0
PFHpS	0.01[b]	0.03[d]	75 (7)	70 (8)	99 (10)	104 (11)	8	8	23	26	+12
L-PFOS	0.02[b]	0.1[e]	81 (7)	72 (6)	100 (6)	100 (7)	11	7	14	6	+3
PFDS	0.005[c]	0.1[e]	74 (10)	70 (8)	165 (25)	157 (17)	9	9	32	31	+118
MeFOSAA	0.003[c]	0.25[e]	99 (18)	77 (9)	89 (18)	97 (11)	8	5	8	10	−12
EtFOSAA	0.003[c]	0.1[e]	111 (28)	68 (10)	85 (9)	94 (9)	10	9	22	18	−12
FOSA	0.01[a]	0.03[d]	73 (7)	75 (5)	80 (5)	90 (7)	7	11	7	8	−7
MeFOSA	0.1[a]	0.3[d]	80 (5)	72 (5)	103 (10)	97 (14)	9	8	11	8	0
EtFOSA	0.04[a]	0.12[d]	78 (8)	68 (5)	107 (14)	95 (5)	7	9	13	8	−7
4:2 FTSA	0.008[c]	0.25[e]	81 (9)	67 (10)	104 (9)	128 (9)	4	10	17	31	−19
6:2 FTSA	0.01[c]	0.25[e]	77 (9)	71 (10)	106 (10)	106 (3)	6	6	8	11	+8
8:2 FTSA	0.03[c]	0.1[e]	72 (8)	76 (7)	92 (20)	82 (3)	3	26	44	44	−10
6:2 diPAP	0.1[a]	0.75[e]	90 (13)	75 (5)	84 (17)	76 (13)	10	6	10	5	+2
8:2 diPAP	0.02[c]	0.75[e]	110 (24)	82 (10)	39 (6)	26 (4)	16	15	24	17	−61
diSAmPAP	0.01[c]	0.75[e]	124 (13)	87 (6)	25 (3)	19 (3)	11	17	41	28	−38

*LOD: limit of detection, determined as follows: (a) when analytes were found in procedural blanks, the LOD was derived from the standard deviation of the blanks multiplied by the $t_{n-1,95}$ student coefficient, n being the number of blank replicates. Otherwise, the LOD was derived from the signal-to-noise ratio (SNR) observed in either low-contaminated seabird plasma samples (b) or in chicken plasma samples spiked at 0.5 ng g^{-1} (c). When two transitions were followed (quantitation and confirmation), the transition with the lowest SNR was chosen to determine the LOD. **LOQ: limit of quantification, set as the more stringent of the two following approaches: (d) 3 × LOD or (e) the lowest point of the linearity range.

Table 3
Comparison of the present method optimized settings and limits of detection (LOD) with previously reported on-line SPE HPLC–MS/MS methods for the analysis of PFASs in plasma samples.

Investigated PFASs	Matrix type	Sample size (μL)	Injection volume (μL)	Loading speed (μL min^{-1})	LOD	Reference
3 (PFOA, PFOS, and FOSA)	*Human Plasma*	300	30	1000	0.05–0.25*	Inoue et al. (2004) [31]
18 (8x PFCAs, 3x PFSAs, 7x FOSA and derivatives)	*Human Serum*	100	400	1000	0.05–0.8*	Kuklenyik et al. (2005) [32]
19 (11x PFCAs, 5x PFSAs, 5x FOSA and derivatives)	*Human Serum*	150	400	NA	0.002–0.05*	Haug et al. (2009) [33]
9 (5x PFCAs, 3x PFSAs, and FOSA)	*Human Serum & Plasma*	100	350	2000	0.009–0.075*	Gosetti et al. (2010) [34]
7 (4x PFCAs, 3x PFSAs)	*Human Serum*	200	200	1000	0.03–0.1*	Mosch et al. (2010) [30]
18 (13x PFCAs, 4x PFSAs, and FOSA)	*Human Cord Blood*	100	20	1500	0.031–0.76*	Llorca et al. (2012) [35]
6 (3x PFCAs, 2x PFSAs, and FOSA)	*Human Serum*	100	60	1500	0.05–0.11*	Bartolomé et al. (2016) [36]
21 (13x PFCAs, 5x PFSAs, 2x Cl-PFESAs and FOSA)	*Human Serum*	25	25	2000	0.008–0.19*	Gao et al. (2016) [37]
12 (6x PFCAs, 3x PFSAs, 3x FOSA and derivatives)	*Human Serum*	50	500	350	0.001–0.006*	Yu et al. (2017) [38]
25 (10x PFCAs, 5x PFSAs) 3x FOSA and derivatives 3x PFPAs, 4x PAPs)	*Human Serum, Plasma, & Whole Blood*	50	80	1500	0.002–0.09*	Poothong et al. (2017) [39]
26 (10x PFCAs, 5x PFSAs, 5x FOSA and derivatives, 3x FTSAs, 2x diPAPs, diSAmPAP)	*Seabird Plasma*	25	400	600	0.003–0.1**	Present study

*LOD expressed in ng mL^{-1}; **LOD expressed in ng g^{-1}.

Table 4
Concentration (ng g^{-1} plasma) in a human serum standard reference material (NIST SRM 1957) determined by the present method at T0 (freshly reconstituted matrix, n = 5) and after six months of storage at − 20 °C (n = 5). When applicable, NIST reference values are also provided.

	Present study (T0)	Present study (T0 + 6 months)	NIST reference values
Replicates	5	5	NA
Unit	ng g^{-1} plasma	ng g^{-1} plasma	ng g^{-1} plasma
PFHpA	0.38 ± 0.05	0.15 ± 0.02	0.31 ± 0.05
PFOA	3.6 ± 0.1	4.2 ± 0.4	5.0 ± 0.4
PFNA	0.79 ± 0.1	0.90 ± 0.07	0.88 ± 0.07
PFDA	0.26 ± 0.02	0.20 ± 0.1	0.39 ± 0.12
PFUnDA	<LOQ	0.21 ± 0.02	0.17 ± 0.04
PFHxS	3.4 ± 0.3	2.9 ± 0.2	4.0 ± 0.8
PFHpS	0.37 ± 0.03	0.34 ± 0.06	NA*
PFOS	21.4 ± 0.6	20.4 ± 1.4	21.1 ± 1.3
MeFOSAA	0.56 ± 0.06	0.75 ± 0.2	NA*

*NA: not available.

in the tropical Indian Ocean or in the temperate North Atlantic and North Pacific waters. Thus, they are likely subject to enhanced PFAS exposure compared to snow petrels that remain within the Antarctic continental shelf (unpublished data). The discrepancy between the PFAS levels observed in the two species may also be attributed to differences in diet such as preying upon different trophic levels [50,51]. These preliminary results provide further evidence of the occurrence of PFASs in biota at global scale, including remote locations such as Subantarctic islands and Antarctica. They also suggest that foraging and migratory habits may play a decisive role in PFAS intake as regards Antarctic seabirds.

4. Conclusions

An automated on-line SPE HPLC–MS/MS method has been developed and validated for the determination of 26 PFASs in various seabird plasma matrixes. The optimization scheme combined experimental designs to select optimal operating conditions, all the while accounting for possible interaction between method parameters. Notably, on-line SPE sample loading volume, flow rate, and final organic solvent percentage were examined to maximize sensitivity performance. The optimization approach implemented conveys important implications for future on-line SPE developments, including other types of environmental and biological matrixes not investigated in the present survey (e.g., water, milk, urine). The optimized settings allowed for the ultra-trace determination of a wider range of PFASs in terms of perfluoroalkyl acid chain lengths (C_4–C_{14}) and precursor chemistries than in previsouly published works. In the present study, additions of isotope-labelled ISs and plasma matrix were operated under strict gravimetric control (weighing). Since this approach did not depend upon the dexterity of the operator or the calibration of micropipettes, it provided a supplementary precision and robustness for more reliable data generation. Environmentally relevant limits of detection were reported (0.003–0.1 ng g^{-1}), lower than or in the same order of magnitude than previous methods that typically employed higher sample volumes [30–35].

The addition of appropriate isotope-labelled ISs at the beginning of the preparation procedure efficiently compensated for potential whole-method recovery losses and matrix effects for most analytes, all the while ensuring accuracy, trueness and precision. The method is robust, allowing the injection of a large number of samples in a single sequence without significant pressure increase or loss of sensitivity, making it eligible for routine analyses. The authors would also like to reiterate the importance of a stringent method validation. In order to endorse conclusions based on plasma/serum biomonitoring surveys, validation endpoints should be carefully ascertained. For instance, a comprehensive matrix effect study across multiple plasma or serum matrixes, as performed in the present survey, would allow to consider a matrix-free calibration approach. In the present work, this was evidenced in the excellent trueness obtained (NIST SRM 1957). After the initial method vali-

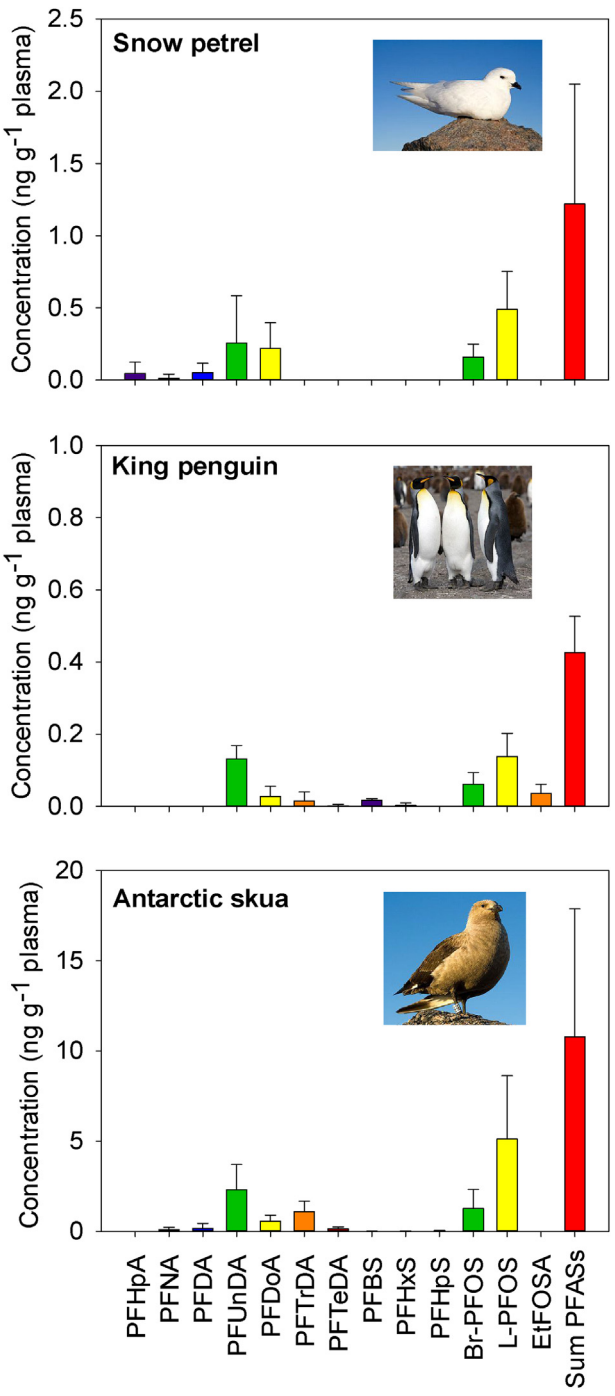

Fig. 4. Average PFAS levels (ng g^{-1} plasma) observed in Antarctic and Subantarctic seabird species (chick-rearing adults for each species). Concentrations are all blank-corrected. Error bars indicate standard deviation (n = 7).

dation, regular monitoring of quality control samples within long sample sequences is an excellent way to verify that no instrumental drift arises over time from the injection of numerous samples; this would ensure a legitimate comparison between samples. One further original aspect of the present work was the investigation of the influence of storage time on method trueness. Due to the remoteness of the sites investigated in the present study, several months typically elapsed between the storage of seabird plasma samples at −20 °C and their reception at the laboratory. Overall, no significant differences appeared between the PFAS concentrations of a freshly reconstituted NIST SRM 1957 human serum sample (T_0) and those after six months of storage at −20 °C (T_0 + 6 months). To the best of the authors' knowledge, this kind of validation is rarely –if ever– studied in the analytical chemistry literature. These preliminary results bear important implications for future large-scale monitoring surveys of PFAS levels in human and wildlife blood/serum, indicating that the validity and reliability of the results would not be overly impacted by initial storage time, at least for the duration examined.

The applicability of the newly-developed on-line SPE HPLC–MS/MS method was assessed through the analysis of adult king penguin, snow petrel and South polar skua plasma samples. Out of the 26 target analytes, 11 were reported in Antarctic seabird plasma samples (ΣPFASs range: 0.37–19 ng g^{-1}), providing further evidence of the ubiquitous dissemination of PFASs in biota. The reduced amount of plasma sample material required (25 μL) also implies that the herein described method could be used to determine PFAS plasma levels in much smaller bird species, as well as in smaller biological models (e.g. zebrafish *Danio rerio*, medaka *Oryzias latipes*) which are frequently the object of ecotoxicology studies.

Acknowledgments

This study was jointly funded by the French National Research Agency (PolarTOP project, grant ANR-10-CESA-0016 to O. Chastel), Institut Polaire Français (program 109 to H. Weimerskirch) and INSU-EC2CO Ecodyn 2014 program (to O. Chastel). The authors also acknowledge funding from the INTERREG ORQUE SUDOE project (SOE3/P2/F591). This study has been carried out with financial support from the French National Research Agency (ANR) in the frame of the "Investments for the future" Program, within the Cluster of Excellence COTE (ANR-10-LABX-45). IdEx Bordeaux (ANR-10-IDEX-03-02) provided the PhD grant allocated to G. Munoz. The Aquitaine Regional Council and the European Union (CPER A2E project) are acknowledged for their financial support. Europe is moving in Aquitaine with the European Regional Development Fund (FEDER).

Appendix A. Supplementary data

Supplementary data associated with this article can be found, in the online version, at http://dx.doi.org/10.1016/j.chroma.2017.07.024.

References

[1] M.P. Krafft, J.G. Riess, Selected physicochemical aspects of poly- and perfluoroalkylated substances relevant to performance, environment and sustainability –Part one, Chemosphere 129 (2015) 4–19.
[2] L. Ahrens, Polyfluoroalkyl compounds in the aquatic environment: a review of their occurrence and fate, J. Environ. Monit. 13 (2011) 20–31.
[3] D. Bertin, P. Labadie, B.J. Ferrari, A. Sapin, J. Garric, O. Geffard, H. Budzinski, M. Babut, Potential exposure routes and accumulation kinetics for poly-and perfluorinated alkyl compounds for a freshwater amphipod: gammarus spp. (Crustacea), Chemosphere 155 (2016) 380–387.
[4] C. Dassuncao, X.C. Hu, X. Zhang, R. Bossi, M. Dam, B. Mikkelsen, E.M. Sunderland, Temporal shifts in poly-and perfluoroalkyl substances (PFASs) in north atlantic pilot whales indicate large contribution of atmospheric precursors, Environ. Sci. Technol. 51 (2017) 4512–4521.
[5] Y. Li, K. Gao, B. Duo, G. Zhang, Z. Cong, Y. Gao, J. Fu, A. Zhang, G. Jiang, Analysis of a broad range of perfluoroalkyl acids in accipiter feathers: method optimization and their occurrence in Nam Co Basin, Tibetan Plateau, Environ. Geochem. Health (2017) 1–10.
[6] Y. Liu, T. Ruan, Y. Lin, A. Liu, M. Yu, R. Liu, M. Meng, Y. Wang, J. Liu, G. Jiang, Chlorinated polyfluoroalkyl ether sulfonic acids in marine organisms from bohai sea, China: occurrence, temporal variations, and trophic transfer behavior, Environ. Sci. Technol. 51 (2017) 4407–4414.
[7] L. Zhang, J. Liu, J. Hu, C. Liu, W. Guo, Q. Wang, H. Wang, The inventory of sources, environmental releases and risk assessment for perfluorooctane sulfonate in China, Environ. Pollut. 165 (2012) 193–198.
[8] X. Dauchy, V. Boiteux, C. Bach, A. Colin, J. Hemard, C. Rosin, J.F. Munoz, Mass flows and fate of per-and polyfluoroalkyl substances (PFASs) in the

wastewater treatment plant of a fluorochemical manufacturing facility, Sci. Total Environ. 576 (2017) 549–558.
[9] S. Newton, R. McMahen, J.A. Stoeckel, M. Chislock, A. Lindstrom, M. Strynar, Novel polyfluorinated compounds identified using high resolution mass spectrometry downstream of manufacturing facilities near Decatur Alabama, Environ. Sci. Technol. 51 (2017) 1544–1552.
[10] K.A. Barzen-Hanson, J.A. Field, Discovery and implications of C2 and C3 perfluoroalkyl sulfonates in aqueous film-forming foams and groundwater, Environ. Sci. Technol. Lett. 2 (2015) 95–99.
[11] S. Mejia-Avendaño, G. Munoz, S. Sauvé, J. Liu, Assessment of the influence of soil characteristics and hydrocarbon fuel cocontamination on the solvent extraction of perfluoroalkyl and polyfluoroalkyl substances, Anal. Chem. 89 (2017) 2539–2546.
[12] G. Munoz, M. Desrosiers, S.V. Duy, P. Labadie, H. Budzinski, J. Liu, S. Sauvé, Environmental occurrence of perfluoroalkyl acids and novel fluorotelomer surfactants in the freshwater fish Catostomus commersonii and sediments following firefighting foam deployment at the Lac-Mégantic railway accident, Environ. Sci. Technol. 51 (2017) 1231–1240.
[13] P. Labadie, M. Chevreuil, Biogeochemical dynamics of perfluorinated alkyl acids and sulfonates in the river seine (Paris, France) under contrasting hydrological conditions, Environ. Pollut. 159 (2011) 3634–3639.
[14] G. Munoz, J.L. Giraudel, F. Botta, F. Lestremau, M.H. Dévier, H. Budzinski, P. Labadie, Spatial distribution and partitioning behavior of selected poly- and perfluoroalkyl substances in freshwater ecosystems: a French nationwide survey, Sci. Total Environ. 517 (2015) 48–56.
[15] C. Lindim, J. Van Gils, I.T. Cousins, Europe-wide estuarine export and surface water concentrations of PFOS and PFOA, Water Res. 103 (2016) 124–132.
[16] N.H. Lam, C.R. Cho, K. Kannan, H.S. Cho, A nationwide survey of perfluorinated alkyl substances in waters, sediment and biota collected from aquatic environment in Vietnam: distributions and bioconcentration profiles, J. Hazard. Mater. 323 (2017) 116–127.
[17] B. González-Gaya, J. Dachs, J.L. Roscales, G. Caballero, B. Jiménez, Perfluoroalkylated substances in the global tropical and subtropical surface oceans, Environ. Sci. Technol. 48 (2014) 13076–13084.
[18] W.A. Gebbink, R. Bossi, F.F. Rigét, A. Rosing-Asvid, C. Sonne, R. Dietz, Observation of emerging per-and polyfluoroalkyl substances (PFASs) in Greenland marine mammals, Chemosphere 144 (2016) 2384–2391.
[19] S. Wild, D. McLagan, M. Schlabach, R. Bossi, D. Hawker, R. Cropp, C.K. King, J.S. Stark, J. Mondon, S.B. Nash, An Antarctic research station as a source of brominated and perfluorinated persistent organic pollutants to the local environment, Environ. Sci. Technol. 49 (2014) 103–112.
[20] C.M. Butt, U. Berger, R. Bossi, G.T. Tomy, Levels and trends of poly-and perfluorinated compounds in the arctic environment, Sci. Total Environ. 408 (2010) 2936–2965.
[21] J.W. Martin, M.M. Smithwick, B.M. Braune, P.F. Hoekstra, D.C.G. Muir, S.A. Mabury, Identification of long-chain perfluorinated acids in biota from the Canadian Arctic, Environ. Sci. Technol. 38 (2004) 373–380.
[22] J. Verreault, M. Houde, G.W. Gabrielsen, U. Berger, M. Haukås, R.J. Letcher, D.C.G. Muir, Perfluorinated alkyl substances in plasma, liver, brain, and eggs of glaucous gulls (Larus hyperboreus) from the Norwegian Arctic, Environ. Sci. Technol. 39 (2005) 7439–7445.
[23] H. Routti, G.W. Gabrielsen, D. Herzke, K.M. Kovacs, C. Lydersen, Spatial and temporal trends in perfluoroalkyl substances (PFASs) in ringed seals (Pusa hispida) from Svalbard, Environ. Pollut. 214 (2016) 230–238.
[24] M. Llorca, M. Farré, M.S. Tavano, B. Alonso, G. Koremblit, D. Barceló, Fate of a broad spectrum of perfluorinated compounds in soils and biota from Tierra del Fuego and Antarctica, Environ. Pollut. 163 (2012) 158–166.
[25] T.H. Nøst, L.B. Helgason, M. Harju, E.S. Heimstad, G.W. Gabrielsen, B.M. Jenssen, Halogenated organic contaminants and their correlations with circulating thyroid hormones in developing Arctic seabirds, Sci. Total Environ. 414 (2012) 248–256.
[26] S. Tartu, G.W. Gabrielsen, P. Blévin, H. Ellis, J.O. Bustnes, D. Herzke, O. Chastel, Endocrine and fitness correlates of long-chain perfluorinated carboxylates exposure in arctic breeding black-legged kittiwakes, Environ. Sci. Technol. 48 (2014) 13504–13510.
[27] K. Kannan, S. Corsolini, J. Falandysz, G. Fillmann, K.S. Kumar, B.G. Loganathan, M.A. Mohd, J. Olivero, N. van Wouwe, J.H. Yang, K.M. Aldous, Perfluorooctanesulfonate and related fluorochemicals in human blood from several countries, Environ. Sci. Technol. 38 (2004) 4489–4495.
[28] K.J. Hansen, L.A. Clemen, M.E. Ellefson, H.O. Johnson, Compound-specific, quantitative characterization of organic fluorochemicals in biological matrices, Environ. Sci. Technol. 35 (2001) 766–770.
[29] S. Huber, J. Brox, An automated high-throughput SPE micro-elution method for perfluoroalkyl substances in human serum, J. Anal. Bioanal. Chem. 407 (2015) 3751.
[30] C. Mosch, M. Kiranoglu, H. Fromme, W. Völkel, Simultaneous quantitation of perfluoroalkyl acids in human serum and breast milk using on-line sample preparation by HPLC column switching coupled to ESI–MS/MS, J. Chromatogr. B 878 (2010) 2652–2658.
[31] K. Inoue, F. Okada, R. Ito, M. Kawaguchi, N. Okanouchi, H. Nakazawa, Determination of perfluorooctane sulfonate, perfluorooctanoate and perfluorooctane sulfonylamide in human plasma by column-switching liquid chromatography-electrospray mass spectrometry coupled with solid-phase extraction, J. Chromatogr. B 810 (2004) 49–56.
[32] Z. Kuklenyik, L.L. Needham, A.M. Calafat, Measurement of 18 perfluorinated organic acids and amides in human serum using on-line solid-phase extraction, Anal. Chem. 77 (2005) 6085–6091.
[33] L.S. Haug, C. Thomsen, G. Becher, A sensitive method for determination of a broad range of perfluorinated compounds in serum suitable for large-scale human biomonitoring, J. Chromatogr. A 1216 (2009) 385–393.
[34] F. Gosetti, U. Chiuminatto, D. Zampieri, E. Mazzucco, E. Robotti, G. Calabrese, M.C. Gennaro, E. Marengo, Determination of perfluorochemicals in biological, environmental and food samples by an automated on-line solid phase extraction ultra high performance liquid chromatography tandem mass spectrometry method, J. Chromatogr. A 1217 (2010) 7864–7872.
[35] M. Llorca, F. Pérez, M. Farré, S. Agramunt, M. Kogevinas, D. Barceló, Analysis of perfluoroalkyl substances in cord blood by turbulent flow chromatography coupled to tandem mass spectrometry, Sci. Total Environ. 433 (2012) 151–160.
[36] M. Bartolomé, A. Gallego-Picó, O. Huetos, M.A. Lucena, A. Castaño, A fast method for analysing six perfluoroalkyl substances in human serum by solid-phase extraction on-line coupled to liquid chromatography tandem mass spectrometry, Anal. Bioanal. Chem. 408 (2016) 2159–2170.
[37] K. Gao, Y. Gao, J. Fu, A. Zhang, A rapid and fully automatic method for the accurate determination of a wide carbon-chain range of per- and polyfluoroalkyl substances (C4–C18) in human serum, J. Chromatrogr. A 1471 (2016) 1–10.
[38] C.H. Yu, B. Patel, M. Palencia, Z.T. Fan, A sensitive and accurate method for the determination of perfluoroalkyl and polyfluoroalkyl substances in human serum using a high performance liquid chromatography-online solid phase extraction-tandem mass spectrometry, J. Chromatrogr. A 1480 (2017) 1–10.
[39] S. Poothong, E. Lundanes, C. Thomsen, L.S. Haug, High throughput online solid phase extraction-ultra high performance liquid chromatography-tandem mass spectrometry method for polyfluoroalkyl phosphate esters perfluoroalkyl phosphonates, and other perfluoroalkyl substances in human serum, plasma, and whole blood, Anal. Chim. Acta 957 (2017) 10–19.
[40] B.L. Joiner, Lurking variables: some examples, Am. Stat. 35 (1981) 227–233.
[41] G. Munoz, S.V. Duy, H. Budzinski, P. Labadie, J. Liu, S. Sauvé, Quantitative analysis of poly- and perfluoroalkyl compounds in water matrices using high resolution mass spectrometry: optimization for a laser diode thermal desorption method, Anal. Chim. Acta 881 (2015) 98–106.
[42] D. Muir, E. Sverko, Analytical methods for PCBs and organochlorine pesticides in environmental monitoring and surveillance: a critical appraisal, Anal. Bioanal. Chem. 386 (2006) 769–789.
[43] S. Rayne, K. Forest, K.J. Friesen, Computational approaches may underestimate pKa values of longer-chain perfluorinated carboxylic acids: implications for assessing environmental and biological effects, J. Environ. Sci. Health Part A 44 (2009) 317–326.
[44] S. Rayne, K. Forest, K.J. Friesen, Extending the semi-empirical PM6 method for carbon oxyacid pKa prediction to sulfonic acids: application towards congener-specific estimates for the environmentally and toxicologically relevant C1 through C8 perfluoroalkyl derivatives, Nat. Prec. (2009).
[45] P.J. Taylor, Review matrix effects: the Achilles heel of quantitative high-performance liquid chromatography–electrospray–tandem mass spectrometry, Clin. Biochem. 38 (2005) 328–334.
[46] R. Vestergren, S. Ullah, I.T. Cousins, U. Berger, A matrix effect-free method for reliable quantification of perfluoroalkyl carboxylic acids and perfluoroalkane sulfonic acids at low parts per trillion levels in dietary samples, J. Chromatogr. A 1237 (2012) 64–71.
[47] P. Labadie, E.M. Hill, Analysis of estrogens in river sediments by liquid chromatography–electrospray ionisation mass spectrometry. Comparison of tandem mass spectrometry and time-of-flight mass spectrometry, J. Chromatrogr. A 1141 (2007) 174–181.
[48] M. Kop, H.U. Peter, O. Mustafa, S. Lisovski, M.S. Ritz, R.A. Phillips, S. Hahn, South polar skuas from single breeding population overwinter in different oceans though show similar migration patterns, Mar. Ecol. Prog. Ser. 435 (2011) 263–267.
[49] H. Weimerskirch, A. Tarroux, O. Chastel, K. Delord, Y. Cherel, S. Descamps, Population-specific wintering distributions of adult south polar skuas over three oceans, Mar. Ecol. Prog. Ser. 538 (2015) 229–237.
[50] C.R. Eklund, Distribution and life history studies of the south-polar skua, Bird-Banding 32 (1961) 187–223.
[51] V. Ridoux, C. Offredo, The diets of five summer breeeding seabirds in Adélie Land, Antartica, Polar Biol. 9 (1989) 137–145.